Damping inertial modes excitation in a closed grid turbulence experiment under rotation

P-P Cortet[1], C Lamriben[1], F Moisy[1] and L R M Maas[2]

[1]Laboratoire FAST, CNRS UMR 7608, Université Paris-Sud, Université Pierre-et-Marie-Curie, Bât. 502, Campus universitaire, 91405 Orsay, France
[1] Royal Netherlands Institute for Sea Research, Texel, The Netherlands

E-mail: ppcortet@fast.u-psud.fr

Abstract. We report an experimental study of the decay of grid-generated turbulence in a confined geometry submitted to a global rotation. Turbulence is generated by rapidly towing a grid in a parallelepipedic water tank. The velocity fields of a large number of independent decays are measured in a vertical plane parallel to the rotation axis using a corotating Particle Image Velocimetry system. We first show that, when a "simple" grid is used, a significant amount of the kinetic energy (typically 50%) is stored in a reproducible flow composed of resonant inertial modes. The possible coupling between these modes and turbulence suggests that turbulence cannot be considered as freely decaying in this configuration. We demonstrate however that these inertial modes may be significantly reduced (down to 15% of the total energy) by adding a set of inner tanks attached to the grid. These results suggest that it is possible to produce an effectively freely decaying rotating turbulence in a confined geometry.

1. Introduction

Translating a grid in a closed volume of fluid is a standard way to generate an approximately homogeneous and isotropic turbulence. Although the level of homogeneity and isotropy of the turbulence generated in this way is not as good as in the more conventional configuration of a fixed grid in an open wind tunnel (1; 2), this closed flow configuration has proved to be very useful when a compact system is needed, and in particular when experiments are performed in a rotating frame (3; 4; 5; 6; 7). Apart from early experiments performed in wind tunnels with a rotating section (8; 9), all rotating grid-generated turbulence experiments since then are based on oscillated or translated grids in closed containers.

In the presence of background rotation, grid-generated turbulence may excite inertial waves. These waves are anisotropic transverse dispersive waves, which propagate through a rotating fluid because of the restoring nature of the Coriolis force (10; 11). Their angular frequency σ lies in the range $[0, 2\Omega]$, where Ω is the rotation rate, indicating that these waves can be excited when the characteristic time of the flow is of order of the rotation period, i.e. when the Rossby number is of order unity. The flow excited by a grid translation is, in general, composed of a superposition of (i) a reproducible flow (determined through ensemble averaging) and (ii) a non-reproducible turbulent flow. During the decay of turbulence, both of these two flow components may excite inertial waves after a certain time, when their characteristic timescale decreases down to the order of the rotation period. The excited inertial waves are respectively (i) reproducible

— and therefore detectable in the ensemble average — and (ii) non-reproducible — detectable in the individual realizations only — and cancel out by phase mixing in the ensemble average since their phase is not coherent between different realizations (12).

If now the rotating grid turbulence experiments are performed in a closed container, inertial waves may appear in the form of standing inertial modes. Inertial modes are the eigenmodes of a given container geometry, and can be found in general when the walls are either normal or parallel to the rotation axis (10; 13; 14). Their resonant frequencies can be derived analytically only in some specific geometries, such as the so-called Kelvin modes in a cylinder rotating about its symmetry axis (15). In the case of a parallelepipedic box, the frequencies and the spatial structure of the inertial modes have been characterized in detail by Maas (16) for an inviscid fluid from numerical simulations.

Reproducible inertial modes excited in grid-generated turbulence have been first observed in a parallelepipedic channel with a free surface by Dalziel (7), who pointed to their potential influence on the decay of the turbulent component of the flow. Inertial oscillations are also clearly visible in the experiments of Morize and Moisy (17) (with a rigid upper surface) and Moisy *et al.* (18) (with a free surface). They have been characterized by Bewley *et al.* (5) in a set of two experiments, in which a grid is rapidly drawn in liquid helium or nitrogen in cylindrical and squared geometries. These authors found good agreement between the measured frequencies and the numerical results of Maas (16) for various aspect ratios. They conclude that translating a grid in a closed rotating container cannot generate freely decaying turbulence, because a significant amount of the initial energy may be first stored in the inertial modes, and then gradually released to the turbulence during the decay. It is noteworthy that in all cases those modes were detected in the ensemble-averaged flow, suggesting that they originate from reproducible flow features and not from turbulence.

The aim of the present paper is to investigate in more details the inertial modes excited when towing a grid in a rotating square container, and to explore to what extent those modes may be reduced. An experimental setup (12) similar to that of Morize *et al.* (4; 17) has been mounted on a new rotating platform, allowing for Particle Image Velocimetry measurements in a vertical plane. We demonstrate that, by attaching a set of inner sidewalls to the grid, the amount of energy stored in the inertial modes may be drastically reduced. A similar configuration has been first shown by Staplehurst *et al.* (6) to reduce significantly the large-scale recirculations in the absence of rotation. We demonstrate here how a configuration inspired from their work strongly reduces the excitation of inertial modes, by an enhanced conversion of the mean flow energy into turbulence.

2. Experimental setup

2.1. Tank and rotating platform

Only the "simple grid" configuration, used in Sec. 3, is described here. The modified configuration with additional inner walls is detailed in Sec. 4.

The experimental setup consists in a cubic glass tank, of lateral side $L = 60$ cm, filled with 52 cm of water (see Fig. 1) and mounted on a precision rotating turntable of 2 m in diameter (11; 12). The angular velocity Ω of the turntable is set to 0.84 rad s^{-1} (8 rpm), with relative fluctuations $\Delta\Omega/\Omega$ less than 5×10^{-4}. The rotation of the fluid is set long before the experiment starts in order for transient spin-up recirculations to be damped and therefore to achieve a solid body rotation. A horizontal cover is placed at a height of $H = 49$ cm, defining the upper boundary of the flow.

Turbulence —and inertial modes— is generated by rapidly towing a square grid at a constant velocity $V_g = 0.70$ m s^{-1} from the bottom to the top of the tank. During the subsequent decay of turbulence, the grid is kept fixed, at a height of 46 cm, slightly below the cover. The grid

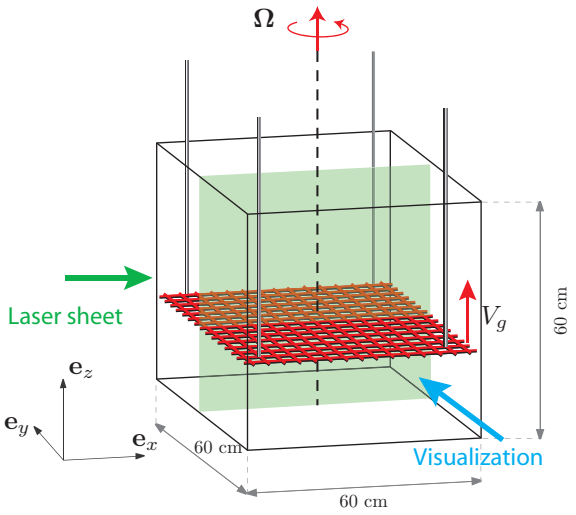

Figure 1. Schematic view of the experimental setup, in the "simple grid" configuration. The $60 \times 60 \times 60$ cm^3 tank is filled with 52 cm of water and is rotating at an angular velocity of $\Omega = 0.84$ rad s^{-1}. A square grid of 40 mm mesh is towed by four shafts from the bottom to the top at constant velocity $V_g = 0.70$ m s^{-1}. PIV measurements in a vertical plane (x, z) are achieved in the rotating frame, based on a laser sheet illuminating the vertical plane (x, z) and a camera aiming normally at it.

consists in 8 mm thick square bars with a mesh size $M = 40$ mm. The grid is rigidly attached at its four corners to a servo-controlled brushless motor ensuring the vertical translation of the grid. The Reynolds number based on the grid mesh is $Re_g = V_g M/\nu = 28\,000$, and the Rossby number is $Ro_g = V_g/2\Omega M = 10.4$, indicating that the flow in the close wake of the grid is fully turbulent and weakly affected by the rotation.

2.2. PIV measurements

Velocity fields in a vertical plane (x, z) are measured using a 2D Particle Image Velocimetry (PIV) system. The flow is seeded with 10 μm tracer particles, and illuminated by a corotating vertical laser sheet passing through the center of the tank. The entire 60×46 cm^2 flow section is imaged through a transparent side of the tank with a double-buffer high-resolution 2048×2048 pixels camera, corotating with the tank and aiming normally at the laser sheet. During the decay of turbulence, 428 image pairs are acquired at a sampling rate of 2 Hz. Since the typical flow velocities decrease with time, the delay between the two successive images of a pair is made to gradually increase during the acquisition sequence, from 10 to 68 ms, so that the typical particles displacement remains constant, of order of 5 pixels, during all the decay. PIV computations are then performed over image pairs, on 32×32 pixels interrogation windows with 50% overlap, leading to a spatial resolution of 4.9 mm.

2.3. Reynolds decomposition

In Fig. 2, we show the time series of the vertical velocity $u_z(x_0, z_0, t)$ at the center of the flow for 20 independent realizations of the decay. The origin $t = 0$ is defined as the time at which the grid reaches the top of the tank. The ensemble average of those realizations is also shown in bold line. This plot clearly illustrates that the flow consists in well-defined oscillations excited by the grid, of characteristic timescale of about one period of rotation, superimposed to non-reproducible turbulent fluctuations. Those oscillations actually correspond to inertial modes, and their amplitude is clearly of the order of the turbulence.

In order to investigate properly the dynamics of the inertial modes and of the turbulence, and the possible coupling between the two, we introduce the standard Reynolds decomposition of the velocity:

$$\mathbf{u}(\mathbf{x}, t) = \mathbf{U}(\mathbf{x}, t) + \mathbf{u}'(\mathbf{x}, t). \tag{1}$$

Here $\mathbf{u}(\mathbf{x}, t)$ is the total velocity field, $\mathbf{U}(\mathbf{x}, t) \equiv \overline{\mathbf{u}}(\mathbf{x}, t)$ its ensemble average (i.e. the

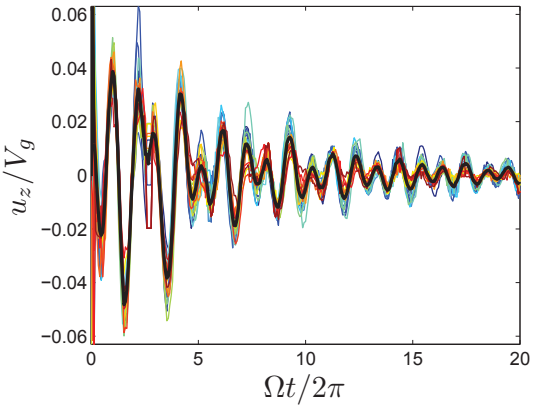

Figure 2. Times series of the vertical velocity $u_z(x_0, z_0, t)$ measured at the center of the flow ($x_0 = 300$ mm, $z_0 = 240$ mm), for 20 realizations performed at $\Omega = 0.84$ rad s^{-1} (in various colors). The black thick line shows the ensemble average of these time series.

reproducible component of the flow) and $\mathbf{u}'(\mathbf{x}, t)$ its turbulent component. The overbar $\overline{\cdot}$ stands for the ensemble average over several independent realizations of the flow. Note that, although the ensemble average is often approximated by a temporal or a spatial average in most turbulence experiments, the use of true ensemble averages here is critical to separate properly the reproducible non-stationary component of the flow from the turbulence.

The Reynolds decomposition (1) naturally leads to introduce three kinetic energies, characterizing the total, ensemble-average (simply denoted "mean" hereafter) and turbulent flows respectively, and defined as:

$$\begin{aligned} k_{tot}(t) &= \langle \overline{\mathbf{u}^2}(\mathbf{x}, t) \rangle, \\ k_{mean}(t) &= \langle \mathbf{U}^2(\mathbf{x}, t) \rangle, \\ k_{turb}(t) &= \langle \overline{\mathbf{u}'^2}(\mathbf{x}, t) \rangle, \end{aligned} \tag{2}$$

satisfying $k_{tot}(t) = k_{mean}(t) + k_{turb}(t)$. Here the brackets $\langle \cdot \rangle$ denote the spatial average over the whole fluid volume.

In practice, only the two velocity components u_x and u_z can be measured, the measurements being restricted to a vertical plane (x, z) located at mid-width of the tank. The measured kinetic energies must therefore be considered as approximations of the true ones. For a statistically homogeneous and isotropic turbulent component, one would simply have $k_{turb}^{mes} = 2k_{turb}/3$. The situation is more complicated for the energy of the mean flow for two reasons: (i) during one period of a given inertial mode, the kinetic energy is basically exchanged between the measured and the non-measured velocity components; (ii) the ratio between the energy averaged over the whole tank and the energy averaged over the measurement plane (x, z) only depends on the details of the spatial structure of each mode, which are not known a priori. For those reasons, we do not apply here any correcting weight to the velocity components when computing kinetic energies, and we simply define

$$k_{tot}(t) = \langle \overline{u_x{}^2}(x, z, t) \rangle_{x,z} + \langle \overline{u_z{}^2}(x, z, t) \rangle_{x,z} \tag{3}$$

(with $\langle \cdot \rangle_{x,z}$ the average over the vertical plane), and similarly for k_{mean} and k_{turb}. Note that those modified definitions still satisfy the relation $k_{tot}(t) = k_{mean}(t) + k_{turb}(t)$.

3. Inertial modes produced by the simple grid configuration

3.1. Kinetic energy decay

In Fig. 3, we present the time evolution of the three kinetic energies (2) computed from 40 decay realizations performed at $\Omega = 0.84$ rad s^{-1}. Both the energy of the total and the mean

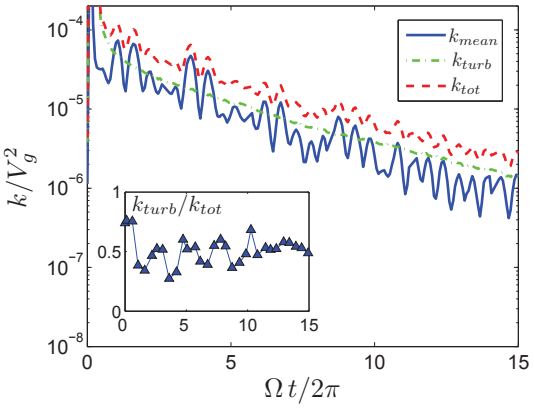

Figure 3. Total (dashed), mean (continuous) and turbulent (dashed-dotted) kinetic energies as a function of the number of tank rotations $\Omega\, t/2\pi$ from 40 realizations performed at $\Omega = 0.84$ rad s^{-1}. Inset: Ratio of turbulent to total kinetic energy α (4), measured at times t_n of maximum mean energy.

flow show, superimposed to their overall decay, marked oscillations corresponding to the inertial modes. On the other hand, the turbulent energy shows a monotonic decrease, suggesting a good separation between the reproducible and non-reproducible components of the flow. At this point, it is important to note that the kinetic energy of the ensemble-averaged flow $k_{mean}(t)$ is of the same order than the turbulent one $k_{turb}(t)$.

The oscillations of $k_{tot}(t)$ and $k_{mean}(t)$ are only due to the 2-dimensions and 2-components restriction of the PIV measurements. Indeed, a monotonic decay should be expected for the true energies (2) computed from the 3 velocity components averaged over the whole fluid volume. We expect therefore that the total and mean kinetic energies are correctly estimated only at the maximum of their oscillations. In order to evaluate the relative amount of turbulent and mean energy in the total flow, we shall therefore consider only the times t_n at which $k_{mean}(t)$ is maximum, and we introduce the ratio:

$$\alpha(t_n) = \frac{k_{turb}(t_n)}{k_{tot}(t_n)}. \tag{4}$$

In the inset of Fig. 3, we actually see that turbulence represents only $50 \pm 10\%$ of the energy in the flow. This quite low ratio indicates that the turbulence produced with this "simple" grid configuration is evenly distributed among the reproducible inertial modes and the "true turbulence". It is therefore questionable to consider this turbulence as freely decaying. Indeed, the possible coupling between the turbulence and the ensemble-averaged flow, which cannot be investigated at this point, may prevent the turbulence to decay freely, as it is continuously fed through energy transfer from the inertial modes.

3.2. Fourier analysis of the inertial modes

In order to characterize in more details the flow generated by the grid translation, we perform a temporal Fourier analysis of the ensemble-averaged flow $\mathbf{U}(\mathbf{x},t) \equiv \overline{\mathbf{u}}(\mathbf{x},t)$. Assuming that this ensemble-averaged flow is composed of inertial modes only, $\mathbf{U}(\mathbf{x},t)$ can be written as follows:

$$\mathbf{U}(\mathbf{x},t) = \Re\left(\sum_{n,m,s} a_{nms}(t)\, \mathbf{v}_{nms}(\mathbf{x})\, e^{i\omega_{nms}t}\right) \tag{5}$$

where $\mathbf{v}_{nms}(\mathbf{x})$ is the (complex) spatial structure of the $[n,m,s]$ mode, ω_{nms} its angular frequency, which lies in the range $[0, 2\Omega]$ allowed for inertial waves, and $\Re$ stands for the real part. With notations similar to that of Maas (16) and Bewley *et al.* (5), we label here the modes using two integer indices, n and m, and a sign, $s = \pm$. The first index n is the normalized vertical wavenumber such that the horizontal (resp. vertical) velocity component has n (resp.

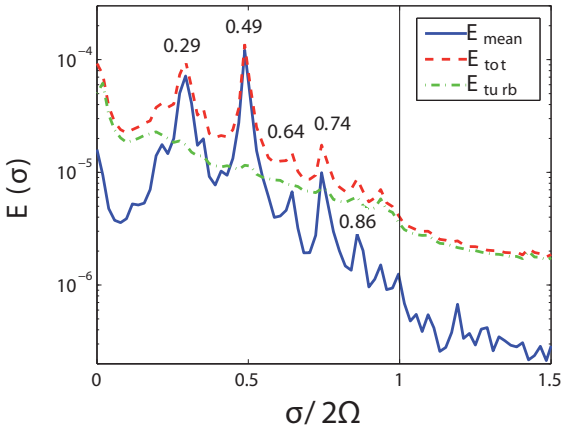

Figure 4. Temporal energy spectrum of the total (dashed), mean (continuous) and turbulent (dashed-dotted) component of the flow as a function of $\sigma/2\Omega$ computed from 40 decay realizations performed at $\Omega = 0.84$ rad s^{-1}, with logarithmic y-axis. Inertial modes can develop for angular frequencies $\sigma < 2\Omega$. The modes corresponding to the peak frequencies are given in Table 1.

$n-1$) nodes in the vertical direction. The horizontal structure of a given mode of vertical index n is characterized by the second index m. Larger values of m essentially correspond to finer structures in the horizontal direction, although it is not directly related to the number of nodes as for the vertical index n. Finally, the sign s refers to the symmetry of the mode with respect to the rotation axis: $s = +$ for a symmetric mode and $s = -$ for an antisymmetric mode. The frequencies ω_{nms} are increasing functions of n and, at fixed n and s, decreasing functions of m. In the absence of coupling with other modes or with turbulence, the amplitude of each mode, $a_{nms}(t)$, is expected to be a decreasing function of time because of viscous damping.

The modes present in the ensemble-averaged flow are identified from the temporal Fourier transform of the ensemble-averaged velocity field $\mathbf{U}$ at each position in the (x, z) measurement plane,

$$\hat{\mathbf{U}}_\sigma(x,z) = \int_{T_{min}}^{T_{max}} \mathbf{U}(x,z,t)\, e^{-i\sigma t}\, dt. \tag{6}$$

The temporal bounds T_{min} and T_{max} have been chosen equal to 1 and 15 rotation periods, respectively. From this, we define the temporal energy spectrum of the mean (ensemble average) flow, spatially averaged over the (x, z) plane, as:

$$E_{mean}(\sigma) = \frac{1}{2\pi}\langle|\hat{\mathbf{U}}_\sigma(x,z)|^2\rangle_{x,z}. \tag{7}$$

In Fig. 4, the spectrum $E_{mean}(\sigma)$ clearly shows a series of peaks, whose values are listed in Table 1. These peak frequencies are in excellent agreement with some of the numerical eigenfrequencies computed (as in Ref. (16)) for our experimental aspect ratio $L/H \simeq 1.22$. This shows that the translation of the grid, because of its specific drag profile, selects only a small set of specific inertial modes among the dense spectrum of modes evidenced in Ref. (16). Those selected modes are among the lowest order modes ($n = 1$ to 3), probably because their simpler structure better matches the spatial features of the ensemble-averaged flow at early times, i.e. before it is affected by rotation, and also because higher order modes decay faster by viscous damping.

In order to check whether the inertial modes are present only in the ensemble-averaged flow, we also introduce the temporal Fourier transform of the total, $\hat{\mathbf{u}}_\sigma(x,z)$, and of the turbulent velocity field, $\hat{\mathbf{u}}'_\sigma(x,z)$, similarly to Eq. (6), from which we can define the corresponding energy

Table 1. Numerical values of normalized frequencies $\sigma/2\Omega$ for different modes of order $[n, m, s]$ (where n is the vertical wavenumber, m characterizes the horizontal structure, and s is the symmetry of the mode) compared to the experimental peaks in Fig. 4. The uncertainty of the experimental values is ± 0.01. The numerical values are computed for an aspect ratio identical to the experimental one $L/H = 1.22$.

mode	$\sigma/2\Omega$	
$[n, m, s]$	num.	exp.
$[1, 4, +]$	0.2992	0.29
$[1, 1, +]$	0.4890	0.49
$[1, 1, -]$	0.6328	0.64
$[2, 1, +]$	0.7429	0.74
$[3, 1, +]$	0.8557	0.86

spectra:

$$E_{tot}(\sigma) = \frac{1}{2\pi}\langle\overline{|\hat{\mathbf{u}}_\sigma|^2}\rangle, \quad (8)$$

$$E_{turb}(\sigma) = \frac{1}{2\pi}\langle\overline{|\hat{\mathbf{u}'}_\sigma|^2}\rangle. \quad (9)$$

As for the kinetic energies, the energy spectra are additive, $E_{tot}(\sigma) = E_{mean}(\sigma) + E_{turb}(\sigma)$. For a given total spectrum $E_{tot}(\sigma)$, the two spectra E_{mean} and E_{turb} allow us to distinguish between two kinds of inertial modes: (i) reproducible (i.e. phase-coherent) modes, characterized by peaks in E_{mean} but not in E_{turb}; (ii) non-reproducible (i.e. random-phase) modes, characterized by peaks in E_{turb} but not in E_{mean}. Interestingly, Fig. 4 shows the complete absence of peaks in the turbulent spectrum $E_{turb}(\sigma)$, indicating that all the inertial modes present in our system are reproducible, and therefore not turbulent. This confirms that inertial modes in this system are more likely excited by reproducible flow features induced by the grid translation. This also suggests that the initial turbulence right after the grid translation is effectively not affected by the rotation, as could be expected from the relatively large grid Rossby number $Ro_g = 10.4$. Therefore, this initial turbulence is expected to be similar to classical grid turbulence in non-rotating systems.

Finally, it is important to note that more than 97% of the energy of the ensemble-averaged flow lies in the range of angular frequencies $[0, 2\Omega]$, confirming that almost all its energy is stored in inertial modes. This result suggests that the ensemble-averaged flow is correctly converged, so that the spectrum of the ensemble-averaged flow is almost not contaminated by the spectrum of residual turbulent fluctuations which spans over larger frequencies. On the contrary, we see that there is a significant amount of energy for $\sigma > 2\Omega$ in the turbulent spectrum, which actually corresponds to the rapid small scales of usual 3D turbulence which are not directly affected by the rotation.

4. Modified configuration with inner walls

4.1. Modified experimental setup

The modified configuration of the experimental setup studied in this section is shown in Fig. 5. It consists in three parallelepipedic PVC tanks, of respective height 50, 40 and 40 cm and width 40, 24 and 8 cm. Each tank consists in 4 vertical sidewalls, without top and bottom walls. The 3 tanks are fit together co-axially, so that two neighbour sidewalls are separated by two grid

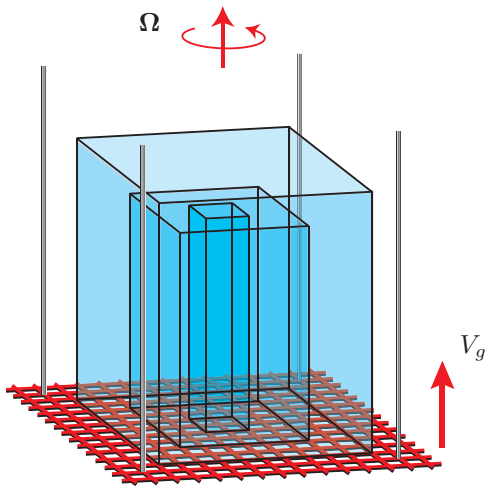

Figure 5. Schematic view of the modified grid configuration (the outer water tank is not shown; see Fig. 1). Three inner tanks are mounted on the grid, and turbulence is generated by raising the set grid+tanks. Each inner tank consists in 4 vertical sidewalls, without top and bottom walls.

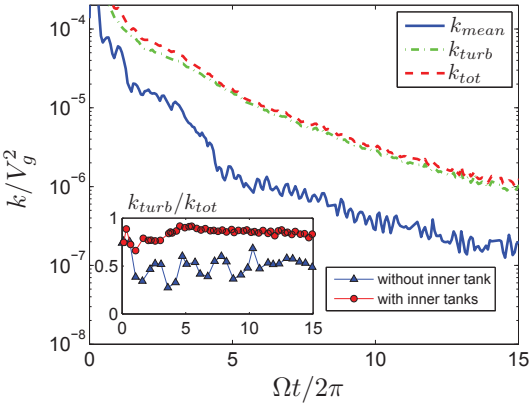

Figure 6. Total (dashed), mean (continuous) and turbulent (dashed-dotted) kinetic energies as a function of reduced time $\Omega t/2\pi$ from 40 decay realizations performed at $\Omega = 0.84$ rad s^{-1} with the modified configuration with inner tanks. Inset: ratio of turbulent to total kinetic energy as a function of reduced time $\Omega t/2\pi$ with (points) and without (triangles) inner tanks.

meshes, and attached on the upper side of the grid. All other parameters, in particular the grid velocity and Rossby number, are the same as for the simple grid configuration. Since our grid is translated from the bottom to the top, here the inner tanks are *upstream* the grid, so that the decaying flow is not confined inside the smallest tank.

The presence of the inner tanks implies that no horizontal cover could be placed to define the upper boundary of the flow, contrarily to the "simple" grid configuration. However, we can consider here that an effective upper boundary is approximately defined by the grid itself, locked at a height of 46 cm after its translation. Indeed, we have checked that the "simple" grid configuration without upper rigid boundary also produces inertial modes, which are as intense as with the rigid boundary. Moreover, here, the inner walls efficiently block the flow in the region between the grid and the free surface.

4.2. Turbulence generated with the grid + inner tanks configuration

The decay of the kinetic energies of the total, mean and turbulent components of the flow as a function of time, from ensemble averages over 40 decay realizations with the modified configuration, is shown in Fig. 6. In comparison with the simple grid configuration (Fig. 3), the oscillations due to the inertial modes are strongly reduced, both for the mean and the total kinetic energies. We also see that, contrary to the simple grid configuration, the turbulent kinetic energy is now significantly larger than the one of the ensemble-averaged flow. This can be better seen in the inset of Fig. 6, showing that turbulence contains, after a transient of about one tank rotation, approximately $85 \pm 5\%$ of the total kinetic energy, a value much larger than

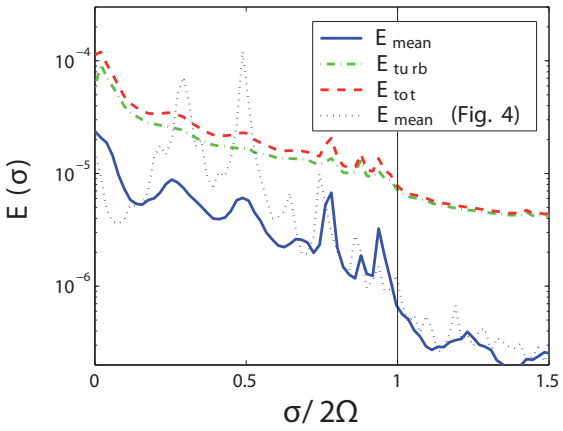

Figure 7. Temporal energy spectrum of the total (dashed), mean (continuous) and turbulent (dashed-dotted) component of the flow as a function of $\sigma/2\Omega$ computed from 40 decay realizations performed at $\Omega = 0.84$ rad s^{-1} with inner tanks with logarithmic y-axis. The dotted line reproduces spectrum of the mean flow for comparison (Fig. 4), obtained with the simple grid configuration.

the 50% obtained with the simple grid configuration.

In Fig. 7, we superimpose the temporal energy spectrum of the mean flow obtained with (continuous line) and without (dotted line) the inner tanks. We clearly see that, with the inner tanks, the two dominant peaks (at $\sigma/2\Omega = 0.29$ and 0.49) have been reduced by more than a factor of 10. The reduction of the other peaks, in particular the $n = 2$ mode at $\sigma/2\Omega \simeq 0.74$, is less pronounced. The decrease of the two dominant inertial modes essentially explains the significant drop of the kinetic energy of the mean flow with respect to turbulence shown in Fig. 6. We can also note slight frequency shifts between the two configurations, probably originating from the not perfectly identical boundary conditions at the top of the container, and hence from slightly different effective aspect ratios.

Interestingly, inertial modes are not only absent from the ensemble-averaged flow spectrum, $E_{mean}(\sigma)$, but also from the turbulent spectrum $E_{turb}(\sigma)$. This indicates that their disappearance in the modified grid configuration cannot be attributed to a change in the nature of the excited inertial modes, from reproducible to non reproducible, but to a true disappearance.

The differences in the energy decays and spectra show that the addition of the inner tanks to the grid leads to a much more efficient transfer of the initial mean flow energy into turbulence, bypassing the generation of inertial modes. However, the origin of the changes between the two configurations is not clear. In particular, it is not evident if, and how, the differences in the grid jet profiles may explain the preferential energy transfer from the mean flow to the turbulence in the modified configuration. These results illustrate the sensitivity of the inertial modes production to slight changes in the grid geometry, at least for the grid Rossby number considered here, $Ro_g = 10.4$.

5. Discussion and conclusion

In this article, we characterize in details the flow generated when a simple grid is rapidly translated in a rotating and confined volume of fluid. We show that, in addition to a non-reproducible turbulent flow, the grid translation initiates a reproducible ensemble-averaged flow composed of resonant inertial modes, which contains a significant amount of the total kinetic energy. This observation agrees with the recent experiments of Bewley *et al.* (5) in a similar geometry. We provide a quantitative comparisons of the mode frequencies with the numerical predictions of Maas (16).

These results suggest that the turbulent (i.e. the non reproducible) component of the flow generated in this configuration cannot be considered as freely decaying. Indeed, energy transfers between the inertial modes and the turbulence may exist, so that the energy initially stored in the

inertial modes may continuously feed the turbulence. However, measuring this transfer would require to compute the turbulent Reynolds stress tensor and its coupling with the ensemble-averaged flow. This cannot be performed from the PIV data presented here, which are limited to two velocity components in a single plane.

The ability of a translated grid to generate or not reproducible inertial waves or modes depends on the grid Rossby number, $Ro_g = V_g/2\Omega M$, and also on the geometrical details of the grid configuration, in particular its solidity (ratio of solid to total area). Indeed, for a given grid geometry, a low Rossby number seems more likely to excite inertial modes, because the reproducible flow structure in the wake of the grid may directly force inertial waves with a phase coherence. On the other hand, we could speculate that, for much larger Rossby numbers (and assuming that the Reynolds number is very large too), the reproducible wake pattern has more time to loose its coherence before being affected by rotation, so its energy may be more efficiently transferred to turbulence than reproducible inertial waves. Even if inertial waves are later generated from these decaying incoherent motions, their random phase should cancel them out by averaging over independant realizations, so inertial modes should not be found in the ensemble-averaged flow.

In the experiments of Bewley *et al.* (5), the moderate grid Rossby number Ro_g of 5.5 is found to produce strong inertial oscillations. In the experiments of Staplehurst *et al.* (6), Ro_g takes even lower values, in the range $1-3.2$, so that significant inertial modes are also expected, although they are not described by these authors. Interestingly, in the present experiment, for a slightly larger grid Rossby number of 10.4, the production of reproducible inertial modes is found to be very sensitive to slight details in the geometry of the grid. Indeed, by adding a set of inner tanks to the grid, we show that it is possible to significantly reduce the production of inertial modes, although the mechanism responsible for this preferred energy transfer towards turbulence instead of modes is not elucidated in the present work. This sensitivity of the flow evidenced for this particular Ro_g is consistent with the results of Morize and Moisy (17), covering a wide range of Ro_g between 2 and 65, in which a smooth transition around $Ro_g \simeq 10$ was found in the decay law of the turbulent energy, suggesting a change in the energy transfer between inertial modes and turbulence.

A first conclusion from these results is that the standard assumption of statistical homogeneity may not be appropriate to describe decaying rotating turbulence in a closed container. This calls for the development of new experiments and theoretical tools to describe the interaction of turbulence with reproducible inertial modes. However, a second conlusion is that, providing the grid Rossby number and the geometrical features of the grid are carefully selected, achieving a nearly "pure" rotating turbulence, free of reproducible inertial modes, is actually possible in a confined geometry. If these requirements are satisfied, this system may be suitable to explore experimentally the influence of the rotation on freely decaying homogeneous turbulence.

Acknowledgments

We acknowledge C. Morize and M. Rabaud for discussions about the manuscript, and A. Aubertin, L. Auffray, C. Borget, G.-J. Michon and R. Pidoux for experimental help. The rotating platform "Gyroflow" was funded by the ANR (grant no. 06-BLAN-0363-01 "HiSpeedPIV"), and the "Triangle de la Physique".

References

[1] Comte-Bellot, G. & Corrsin, S. 1966 The use of a contraction to improve the isotropy of grid-generated turbulence. *J. Fluid Mech.* **65**, 657.

[2] Mohamed, S. & LaRue, J. 1990 The decay power law in grid-generated turbulence. *J. Fluid Mech.* **219**, 195.

[3] Ibbetson, A. & Tritton, D. 1975 Experiments on turbulence in a rotating fluid. *J. Fluid Mech.* **68**, 639.

[4] Morize, C., Moisy, F. & Rabaud, M. 2005 Decaying grid-generated turbulence in a rotating tank. *Phys. Fluids* **17**(9), 095105.

[5] Bewley, G. P., Lathrop, D. P., Maas, L. R. M. & Sreenivasan, K. R. 2007 Inertial waves in rotating grid turbulence. *Phys. Fluids* **19**, 071701.

[6] Staplehurst, P. J., Davidson, P. A. & Dalziel, S. B. 2008 Structure formation in homogeneous freely decaying rotating turbulence. *J. Fluid Mech.* **598**, 81.

[7] Dalziel, S. B. 1992 Decay of rotating turbulence: some particle tracking experiments. *Appl. Sci. Research* **49**, 217–244.

[8] Wigeland, R. A. & Nagib, H. M. 1978 Effects of rotation on decay of turbulence. *Bull. Am. Phys. Soc.* **23** (8), 998.

[9] Jacquin, L., Leuchter, O., Cambon, C. & Mathieu, J. 1990 Homogeneous turbulence in the presence of rotation. *J. Fluid Mech.* **220**, 1.

[10] Greenspan, H. 1968 *The theory of rotating fluids* Cambridge University Press, London.

[11] Cortet, P. P., Lamriben, C. & Moisy, F. 2010 Viscous spreading of an inertial wave beam in a rotating fluid. *Phys. Fluids* **22**, 086603.

[12] Lamriben, C., Cortet, P. P., Moisy, F. & Maas, L. R. M. 2011 Excitation of inertial modes in a closed grid turbulence experiment under rotation. *Phys. Fluids* **23**, 015102.

[13] Fultz, D. 1959 A note on overstability and the elastoid-inertia oscillations of Kelvin, Solberg, and Bjerknes. *J. Meteorol.* **16**, 199.

[14] McEwan, A. D. 1970 Inertial oscillations in a rotating fluid cylinder. *J. Fluid Mech.* **40**, 603.

[15] Batchelor, G. K. 1967 *An Introduction to Fluid Dynamics* Cambridge University Press, Cambridge.

[16] Maas, L. R. M. 2003 On the amphidromic structure of inertial waves in a rectangular parallelepiped. *Fluid Dyn. Res.* **33**, 373.

[17] Morize, C. & Moisy, F. 2006 Energy decay of rotating turbulence with confinement effects. *Phys. Fluids* **18** (9), 065107.

[18] Moisy, F., Morize, C., Rabaud, M. & Sommeria, J. 2010 Decay laws, anisotropy and cyclone-anticyclone asymmetry in decaying rotating turbulence. *J. Fluid Mech.* **664**, 5.